OPTIMIZATION OF MOLDING MATERIAL COMPOSITION FOR IMPROVED HARDNESS IN SAND-CAST ALUMINUM ALLOYS USING METAL CHIPS: TAGUCHI DESIGN APPROACH

Maaruf Isyaku[a], Danjuma Saleh Yawas[ab], Mathew Olatunde Afolayan[a], Terva Ause[c], Tanimu Kogi Ibrahim[d*]

[a]Mechanical Engineering Department, Ahmadu Bello University, Zaria, Nigeria
[b]Shell JV Professorial Chair Office, Mechanical Engineering Department, Ahmadu Bello University, Zaria, Nigeria
[c]Metallurgical and Materials Engineering Department, Ahmadu Bello University, Zaria, Nigeria
[d]Department of Mechanical Engineering, Federal University Wukari, Nigeria.

[*]Corresponding email: terrytanimu@gmail.com

Article history
Received
26th August 2025
Revised
17thNovember 2025
Accepted
31st January 2026
Published
2nd June 2026

ABSTRACT

This study presents an innovative and environmentally friendly method for enhancing the hardness and thermal stability of aluminum alloy castings by incorporating metallic machining chips into foundry sand. The research identifies the optimal combination of parameters using Taguchi optimization and regression modeling. Characterization techniques, including X-ray fluorescence (XRF), thermogravimetric analysis (TGA/DTA), scanning electron microscopy (SEM), and optical microscopy, were employed to validate the results. XRF analysis confirmed that the base aluminum alloy (engine block) contained aluminum, silicon, and magnesium, while brown sand consisted mainly of silicon, phosphorus, and potassium. Cast iron and brass chips contained iron, carbon, silicon, copper, zinc, and iron, respectively. Mechanical testing revealed a 21.2% improvement in the hardness of the modified aluminum alloy over the as-cast sample. Taguchi optimization identified the optimal conditions as brass chip type (level 4), 30 wt% content (level 3), and 100 µm particle size (level 1), which yielded a 26.08% increase in hardness. SEM and optical microscopy of the optimal sample showed significant grain refinement compared to the control. TGA/DTA results demonstrated a 12.99% increase in residual mass and a 28.37% improvement in thermal degradation resistance, indicating better thermal stability. The regression model developed for predicting hardness exhibited strong performance, with R^2, adjusted R^2, and predicted R^2 values of 97.81%, 96.35%, and 91.33%, respectively. Foundry tests further revealed 16.03%, 18.18%, and 6.82% improvements in green compressive strength, dry compressive strength, and compactibility, respectively, for brass chip-modified sand. These findings have significant implications for foundry operations. The integration of metallic machining chips into conventional sand molds can be practically adopted as a cost-effective and sustainable technique to enhance the mechanical properties of aluminum alloy castings without altering the alloy composition

Keywords: *Hardness Improvement, Metallic Chips Reinforcement, Foundry Sand Modification, Aluminum Alloy Casting, Taguchi Optimization, Thermal Stability*

1.0 INTRODUCTION

The mechanical integrity and surface performance of a cast engineering component are primarily determined by its hardness. This critical property defines the material's resistance to localized plastic deformation, abrasion, wear, and indentation [1]. In practical applications such as engine components, machine parts, and structural castings, the durability and wear life of the materials are critically dependent on hardness. In sand-cast aluminum alloys, particularly A356, the slow cooling rate of conventional sand molds results in coarse grains, which compromise both hardness and surface performance. Recent research confirms that optimizing sand grain size, moisture content, and pouring temperature [2], adopting advanced cooling methods such as ablation casting [3], or using novel Al–La–B grain refiners can significantly refine the microstructure, thereby improving hardness, tensile strength, and wear resistance [4].

Hardness is influenced by several metallurgical factors, chief among them being the grain structure of the cast metal. The formation of fine grains during solidification has been consistently linked to higher hardness values, improved wear resistance, and enhanced overall mechanical behavior. Grain refinement techniques, therefore, play an essential role in optimizing the hardness of cast components [4-5]. While chemical grain refiners, external agitation, and electromagnetic stirring have been explored in past studies, these methods often have significant economic, technical, and environmental drawbacks. A more sustainable and economically viable method is required, particularly for local foundries and small- to medium-scale industries [2,5].

This study introduces an innovative and environmentally conscious technique to enhance hardness in aluminum alloy castings by modifying the mold composition used during sand casting. Specifically, the research investigates the effects of incorporating metal chips derived from brass and cast iron machining waste into traditional molding sand. This approach is not only geared toward improving the thermal conductivity of the mold, thereby refining the grain structure and enhancing hardness, but also promotes responsible waste reuse and sustainable manufacturing practices in alignment with the United Nations Sustainable Development Goals (SDGs): SDG 9 (Industry, Innovation, and Infrastructure), SDG 12 (Responsible Consumption and Production), and SDG 13 (Climate Action) [6-8].

Traditionally, sand casting has been widely adopted for its simplicity, low cost, and flexibility in producing complex shapes. However, one of its significant limitations lies in the insulating nature of silica sand, which leads to slow heat extraction during solidification. This results in the formation of coarse grains, which directly contribute to low hardness, poor wear resistance, and reduced surface quality of the final product. Consequently, cast components made by sand casting often require secondary operations such as heat treatment or surface hardening, which increase production time and cost. The current research seeks to mitigate this limitation by exploring a proactive approach to enhance hardness at the casting stage itself [9-12].

The idea of adding metal chips to the sand mold is based on their superior thermal conductivity relative to silica sand. By embedding metallic particles within the molding sand, the heat transfer rate from the molten metal to the surroundings is significantly improved, leading to rapid cooling and finer grain formation. Fine-grained aluminum alloys exhibit increased resistance to indentation, making them suitable for applications where surface hardness and wear resistance are critical. Additionally, by utilizing discarded brass and cast iron chips, the process introduces a circular economy model into foundry operations, thereby reducing environmental pollution caused by metal waste [13-14].

This approach not only targets improved mechanical performance but also addresses a significant environmental challenge: the indiscriminate disposal of metal chips from machine shops, automotive garages, and manufacturing industries. When dumped on soil, water bodies, or public spaces, metal chips contribute to soil degradation, water pollution, and health risks for humans and animals [15]. Their reintegration into molding

sand transforms what would otherwise be pollutants into resources, promoting SDG 12 by encouraging responsible consumption and sustainable production practices [7,16-18].

From an engineering and metallurgical standpoint, hardness is a critical property for ensuring a component's resistance to wear, particularly in dynamic applications such as pistons, valves, brake rotors, engine blocks, and connecting rods. Components subjected to continuous rubbing, sliding, or compressive forces must possess sufficient hardness to withstand prolonged usage without excessive material loss. Inadequate hardness leads to rapid deterioration, necessitating frequent replacement and higher operational costs. By enhancing the hardness at the microstructural level during casting, this study aims to minimize the need for post-processing while improving component longevity [19-20].

Moreover, the innovation contributes to SDG 9 by promoting inclusive and sustainable industrial development through the use of accessible and low-cost technologies [7]. In many developing nations, foundry operations are labor-intensive and limited in technological advancement. By adopting a simple method for incorporating metal chips into sand molds, foundries can significantly enhance the performance of their castings without incurring substantial capital investment. The approach is particularly beneficial for countries like Nigeria, which, according to the Raw Materials Research and Development Council (RMRDC), hosts more than 50 foundries with a combined annual casting capacity of over 80,000 tons. Improving the quality of cast products from these foundries has the potential to boost local manufacturing, reduce import dependency, and create sustainable industrial value chains [21].

The theoretical basis for hardness enhancement through grain refinement lies in the Hall–Petch relationship, which describes how the reduction in grain size leads to an increase in the strength and hardness of a material [22-23]. Smaller grains mean more grain boundaries, which act as barriers to dislocation motion, thereby improving resistance to deformation under applied stress. A finer and more uniform grain structure can be achieved by ensuring rapid solidification through improved mold thermal conductivity. In aluminum alloys, this translates to a more complicated, tougher, and more durable casting [24].

Experimentally, this research utilizes aluminum alloys cast in molds prepared with varying proportions of brass and cast iron chips mixed with foundry-grade silica sand. The Taguchi method is used for experimental design, allowing the investigation of multiple parameters, including chip percentage, chip type, and particle size. Standard Brinell and Rockwell hardness tests are employed to quantify the hardness of the cast components. At the same time, microstructural analysis via optical and scanning electron microscopy provides insights into grain size distribution and morphology. The results are then analyzed using regression models and grey relational analysis to identify optimal mold compositions for maximum hardness.

This research also contributes to SDG 13 by reducing the carbon footprint of metal casting. The conventional methods for grain refinement and hardness improvement, such as chemical additions and heat treatment, require substantial energy input and may involve hazardous chemicals. In contrast, the proposed technique utilizes pre-existing waste materials and enhances mechanical properties through physical means (heat conduction), resulting in lower energy consumption and fewer emissions. Moreover, increased hardness extends component lifespan, reducing the frequency of replacement and the associated environmental costs of remanufacturing.

Beyond the technical advantages, the approach also supports local economic development by providing small-scale foundries with a competitive edge. Improved component performance results in enhanced product quality, increased customer satisfaction, and improved marketability. Additionally, reducing waste and improving energy efficiency translates into lower production costs, thus empowering local industries to thrive in a sustainable manner.

This study presents a novel and practical solution to one of the fundamental limitations of sand casting, namely, low hardness due to coarse grains, by incorporating

metal chips as additives into the molding material. The technique not only improves the mechanical performance of cast aluminum alloys but also promotes environmental sustainability, economic efficiency, and industrial innovation. By aligning with SDGs 9, 12, and 13, the research exemplifies how engineering advancements can be harnessed to address both technical and global sustainability challenges. The findings of this investigation have the potential to redefine best practices in sand casting and encourage wider adoption of sustainable metallurgical methods across the foundry industry.

2.0 EXPERIMENTAL PROCEDURE

2.1 Materials

The materials used in this work include: a used engine block, obtained from Pantaka Market; Kaduna spare parts/scraps along the Kaduna western by-pass, Kaduna State, Nigeria; foundry sand and bentonite; machined chips of gray cast iron; chips of brass; grinding papers, polishing cloth and powder, cotton cool, and etchant.

2.2 Collection of samples

Cast iron chips were collected from an automobile workshop in Tudun Wada, Zaria. These chips were obtained from the re-boring of engine blocks of 10-seater Toyota buses. The engine blocks were made of cast iron.

Discontinuous brass chips were obtained from a machining shop in Panteka Market in Kaduna, while the sand used for this research work was from Zaria Dam in Ahmadu Bello University.

2.3 Sieving of the collected metal chips and molding sand

The sand and metal chips were sieved using a vibrating sieve shaking machine in the foundry workshop of the Metallurgical and Materials Engineering Department, Ahmadu Bello University, Zaria. The grain size of sand is usually expressed by a "grain fineness number." A given grain fineness number corresponds to a standard sieve of 200 mm diameter, which has an identical number of meshes on it. To determine this number for a given sand sample, it is customary to use a standard sieve placed above each other, whereby the coarsest sieve is placed at the top while the finest is at the bottom.

As specified by the American Foundry Society (AFS) standard, 100g of the sand was weighed and placed/poured onto the topmost sieve (the coarsest) and then placed on the set of sieves on the sieve shaking machine. The machine was switched on and allowed to shake/vibrate for 20 minutes, after which the sieves were removed from top to bottom, and the sand retained/contained in each was weighed and tabulated. The weight collected from each sieve was multiplied by the mesh number, and the total product was divided by the total sample weight to obtain the fineness number [25]. The result of the sieve analysis of the sand is shown in Table 1.

Table 1: The result of the sieve analysis of the Silica Sand

S/n	Mesh Size (mm)	Weight Retained
1	1.4	-
2	1.0	-
3	0.71	0.4
4	0.50	12.33
5	0.35	43.30
6	0.25	31.12
7	0.180	6.27
8	0.125	3.38

9	0.09	1.09
10	0.063	1.05
11	PAN	0.91
12	Total	99.85

Notes: total weight of sample = 100g; time of shaking = 15mins

2.4 Planning Experiment Runs

The Taguchi design approach was used to plan experimental runs using Minitab Statistical Software. This study considered three factors (type of chips, chip content, and chip particle size) and four levels, as shown in Table 2, which gives the standard Taguchi L_{16} orthogonal array design as shown in Table 3.

Where 1= cast iron chips, 2= brass chips and cast iron chips (1:2), 3= brass chips and cast iron chips (2:1), and 4= brass chips,

Table 2: Sand Mold Parameters and Their Levels for the Production of Aluminum Alloy

S/N	Processing Factors	Factors Designation	Level			
			1	**2**	**3**	**4**
1	Chip Type	A	1	2	3	4
2	Chip Content (%)	B	10	20	30	40
3	Chip Particle Size (µm)	C	100	200	300	400

Table 3: L_{16} Orthogonal Array of Sand Mold Composition for Aluminium Alloy Production

Runs	**Factors**			**Responses**
	A	**B (wt%)**	**C(µm)**	**Hardness**
1	1	1	1	
2	1	2	2	
3	1	3	3	
4	1	4	4	
5	2	1	2	
6	2	2	1	
7	2	3	4	
8	2	4	3	
9	3	1	3	
10	3	2	4	
11	3	3	1	
12	3	4	2	
13	4	1	4	
14	4	2	3	
15	4	3	2	
16	4	4	1	

2.5 Mixing of Various Blends

The various blends of molding sand were produced by mixing the sand with various proportions of the metal chips of different particle sizes, using the specifications given by

each experimental run in Table 3. The sand and the chips were measured using a digital weighing machine and poured onto the metallic table. Sand blinder (2% Bentonite) was measured and poured on top of the mixture on the metallic table, and 5 % water was added, after which thorough mixing was carried out using an electromechanical mixing machine within 5 minutes in order to avoid loss of water content by drying due to evaporation. Molding sand without chips was also made using 2% bentonite and 5% water; this mixture was considered the control sample since it contained no metal chips. Hence, the casting produced from it will be compared with the ones with metal chip blends.

2.6 Molding Procedure for Production of Aluminum Alloy

A cylindrical pattern of 15 mm diameter and 300 mm length was made using a stainless-steel pipe to have enough length and diameter of the cast product for various mechanical tests.

The molding box was placed in a position, and then a small quantity of the molding mixture was poured into it and rammed to a height of 20 mm from the base of the box. The cylindrical pattern was then positioned over the rammed base. More molding mixture was poured into the box until it was filled. More ramming was made until proper compaction was achieved. The excess molding sand over the molding box was removed after final ramming. The pattern was withdrawn vertically and carefully from the molding box, creating the designed cavity.

2.7 Melting and Casting

The source of the aluminum alloy melted in the experiment was an automobile engine block, which was broken into pieces for easier charging into the charcoal-fired crucible furnace. A medium-sized crucible pot was chosen based on the volume of the cavities for the casting. The crucible furnace was set up and fired for about 30 minutes, and the aluminum alloy was charged until melting began.

Melting was continued with increased firing of the furnace until a temperature of 804 °C (above the melting point of aluminum alloy) was attained according to the method of Kang *et al.* [26]. This temperature was attained to ensure fluidity. The firing was then reduced until the temperature dropped to 720 °C (close to the melting point of aluminum alloy) when pouring of the molten aluminum alloy into the mold cavity began.

After pouring and filling all the cavities in the mold, the casting was allowed to solidify and cool to room temperature before shaking out and removing the cast bars. The cast bars were collected and labeled according to the various blends. Figure 1 shows some of the casting processes.

Figure 1: Casting Processes of the Aluminium Alloy

2.8 Production of standard test samples from the optimal formulated molding sand for evaluation of foundry properties

From the formulation, some sets of cylindrical-shaped test samples of standard dimensions of 5cm (height) and 5cm (diameter) were produced after the ramming operation by applying three blows on the ramming machine (shown in Figure 2(a). Figure 2(b) shows the cylindrical-shaped molded test sample produced.

2.8.1 Green compression strength test

A standard universal sand strength test machine was used. The produced samples were fixed on the strength testing machine using a compression–holding device as shown in Figure 2(c). This test was carried out according to a uniformly increasing load of 5 KN, which was applied to the specimen by rotating the machine's lever clockwise until the specimen was crushed. The point on the scale at which the specimen was crushed was read and recorded as the compression strength. This test was conducted according to the method of Seidu & Kutelu [9].

2.8.2 Dry compression strength test

The standard green test samples produced were taken and placed inside the oven and baked at 1100C for 1 hour, then removed and cooled; each of the cooled samples was taken and fixed on the strength testing machine, and the same procedure used for the green compression test stated in Section 2.8.1 was followed, after which the result obtained was recorded.

2.8.3 Compactibility test

The standard specimen in the tube was placed in position in the rammer machine for five consecutive blows as the standard for the machine. A weight of 6.35 kg of the rammer was used to give the five blows of the rammer head on the specimen. The movement between the fourth and fifth blows was taken from the scales of values assigned to this movement, with zero travel corresponding to maximum compactibility. The test was carried out for all the molding sand mixtures formulated.

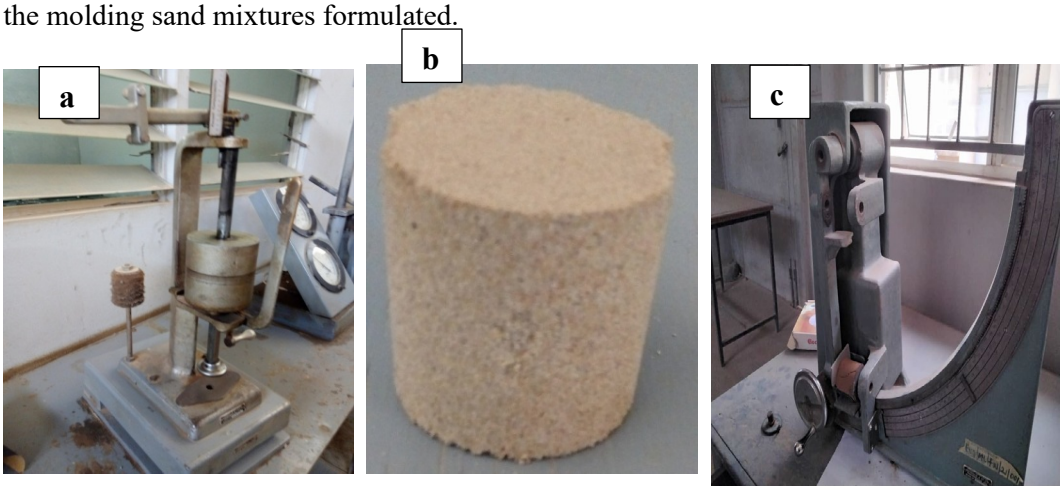

Figure 2: Standard Sand Rammer (a), Sample Produce (b), and Sand Strength Testing Machine(c)

2.9 Machining of the cast bars into standard test samples

The cast cylindrical Aluminium alloy bars were cut and machined to standard test samples for hardness and microstructural tests. The samples were machined on a lathe machine in the workshop of the Mechanical Engineering Department, Ahmadu Bello University, Zaria. The machined samples were then subjected to the following tests.

2.10 Hardness test

The Brinell Hardness test was conducted in the Materials Testing Laboratory of the Department of Metallurgical and Materials Engineering, Ahmadu Bello University, Zaria.

The Hardness of the cast samples was obtained using a Brinell hardness tester. The hardness test samples were prepared to standard dimensions as specified in ASTM A370 (2007). The hardness test was carried out at three points on each test sample, and the average value was recorded. Before the hardness was measured, the samples were subjected to metallographic sample preparation processes of successive grinding on emery papers followed by polishing.

2.11 Metallographic (Microstructural) examination

The microstructures were obtained using the optical microscope in the Department of Metallurgical and Materials Engineering at Ahmadu Bello University, Zaria.

Polishing was carried out on two 15cm diameter rotating discs of the METASERV universal polishing machine with synthetic velvet polishing cloths impregnated with 1-micron Alumina paste. The samples were etched using a solution containing 5 mL of nitric acid, 2 mL of hydrofluoric acid, and 100 mL of distilled water for 10 seconds. The samples were then taken to a scanning electron microscope (SEM) machine, whereby the SEM structures were observed and taken [27-29].

2.12 Optimization and Regression Analysis Procedure

With the aid of Minitab and Origin (Version 2020, OriginLab) software, the experimental properties of the developed aluminum alloy were analyzed using the Taguchi optimization approach and regression analysis [30].

2.13 Taguchi optimization

A common technique for assessing the strength of the connection between sequences is based on the signal-to-noise ratio, which was generated using the Taguchi approach. The Taguchi method divides the S/N ratio into three categories: nominal-the-better, higher-the-better, and lower-the-better [31-32].

The lower-the-better and higher-the-better criterion linear data pre-processing methods were utilized in this study for the properties of the examined aluminum alloy based on the S/N ratio (η) function, which is given in Equations 1 and 2, respectively [33-35].

$$\eta = -10\log_{10}\left(\frac{1}{n}\sum_{i=1}^{n} y_i^2\right) \quad (1)$$

$$\eta = -10\log_{10}\left(\frac{1}{n}\sum_{i=1}^{n} \frac{1}{y_i^2}\right) \quad (2)$$

Where n is the sample size, and yi is the response of the run.

2.14 Confirmation experiment

The confirmation experiment was conducted at the optimum settings to verify the quality characteristics of the hardness predicted at the optimum conditions. To validate the Taguchi predicted optimum conditions, a new aluminum alloy using the optimum levels of the factors was cast, and a confirmation test was performed per ASTM standard on the produced sample with three replications [36].

2.15 Estimating the optimal values

The predicted optimum value of the means or S/N ratio (T_{opt}) of the response was determined by Equation 3 [37].

$$T_{opt} = T_m + \sum_{k=1}^{k_n}\left[(T_{ij})_{max} - T_m\right] \quad (3)$$

Where: T_m is the overall mean or S/N ratio; $(T_{ij})_{max}$ is the mean or S/N ratio of the optimum level (i) of factor k, and k_n is the number of main design factors that affect the response.

T_{ijmax} is obtained from the main effect graph of mean or S/N ratio for each parameter; the highest value among the levels is the $(T_{ij})_{max}$.

2.16 Confidence Interval (CI)

For this study, the experimental value is expected to fall within this range shown below;

Predictive – CI< Experimental< Predictive +CI

Where predictive is the predicted or optimum hardness, experimental is the experimental value after the confirmation test, while CI is the Confidence Interval. Equation 4 was used to evaluate the confidence interval [38].

$$C.I. = \sqrt{f_{\propto(1,d_e)} v_e \left(\frac{1}{U} + \frac{1}{W}\right)} \quad (4)$$

Where $f_{\propto(1,\,d_e)}$ is the F Distribution Critical Values of F (α=5% significance level) (obtained from statistical tables) between 1 and d_e,(which is the degree of freedom of error) obtained from the analysis of variance, v_e is the variance (mean square) of error from the regression table. W is the number of effective replications = 3. U was calculated using Equation 5 [39].

$$U = \frac{Total\ number\ of\ experiment}{1 + degree\ of\ freedom\ of\ control\ Factor} \quad (5)$$

2.17 Regression Analysis (modeling)

Linear regression analysis was performed using Minitab software. This analysis generated an ANOVA table (including interactions), showing each processing parameter's significance level. It was used to develop the predictive mathematical model for all the responses as a function of the process parameters.

3.0 RESULTS AND DISCUSSION

3.1 XRF for the chemical composition of sand, brass, cast iron, and aluminum alloy

The XRF analysis results for the sand, brass, cast iron, and aluminum alloy (scrap engine top cylinder) are presented in Tables 4 to 7. The analysis revealed the dominant elements in each material used for sand mold reinforcement and aluminium alloy for casting. The aluminum alloy in Table 4 primarily consists of aluminum (76.61%), silicon (17.49%), and copper (1.90%), typical of Al–Si alloys, with copper contributing to enhanced strength and fatigue resistance. The brown sand in Table 5 is composed mainly of silicon (89.51%), along with phosphorus (7.41%) and potassium (1.70%), indicating high silica content and favorable thermal stability. Cast iron chips in Table 6, rich in iron (88.3%), carbon (3.7%), and silicon (2.8%) offer excellent thermal conductivity and heat retention, aiding faster and more uniform solidification. Likewise, brass chips in Table 7, composed of copper (64.00%), zinc (23.00%), and iron (3.20%), enhance thermal transfer within the mold due to copper's high conductivity. Adding these metallic chips into the sand matrix improves heat extraction during casting, resulting in finer microstructures and superior mechanical properties in the aluminum alloy.

Table 4: Elemental Composition of the Aluminum Alloy Sample

Element	Mg	Al	Si	S	Ca	Ti	Cr	Mn	Fe	Ni	Cu	Zn	Ba	Pb
%	1.28	76.61	17.49	0.15	0.09	0.03	0.07	0.20	1.14	0.07	1.90	0.85	0.02	0.06

Table 5: Elemental Composition of Brown Sand Sample

Element	Si	Al	P	Cl	K	Ca	Ti	Fe	Rb	Sr	Zr
%	89.51	0.43	7.41	0.07	1.7	0.11	0.05	0.7	0.01	0.01	0.02

Table 6: Elemental Composition of Cast Iron Sample

Element	Fe	C	Si	Al	Ca	Ag	Ca	K	Na
%	88.3	3.7	2.8	1.1	0.7	0.8	0.5	0.3	1.1

Table 7: Elemental Composition of Brass Sample

Element	Cu	Zn	Pb	Fe	Sn	Ca	Ti	K	Mn
%	64	23	2.1	3.2	1.34	2.18	1.51	1.55	1.02

3.2 Aluminium Alloy Hardness Test Results

Table 8 presents the results of the hardness test and its signal-to-noise ratio, as well as those of the control (as cast aluminium alloy). From the table, the highest hardness of 80 R_B was recorded at experiments No. 11, 15, and 16, and the minimum of 68 R_B was recorded at experiment No. 8. As shown in the table, the hardness value of the as-cast aluminum alloy (66 R_B) is lower than that of the 16-produced aluminium alloy. This could be attributed to grain refinement due to an increased cooling rate. The results agree with work carried out by Ali *et al.* [40], using ultra-high-strength steels, who found an increase in hardness, yield strength, and ultimate tensile strength due to grain refinement.

Table 8: Orthogonal Array (Factors and Levels), Response, and S/N Ratio

Runs	Factors			Hardness Value	
	Chips Type	Chips Content (wt%)	Chips Size (µm)	Mean (R_B)	S/N (dB)
1	1	10	100	71	37
2	1	20	200	70	36.9
3	1	30	300	69	36.8
4	1	40	400	70	36.9
5	2	10	200	73	37.3
6	2	20	100	76	37.6
7	2	30	400	74	37.4
8	2	40	300	68	36.7
9	3	10	300	74	37.4
10	3	20	400	75	37.5
11	3	30	100	80	38.1
12	3	40	200	73	37.3

13	4	10	400	77	37.7
14	4	20	300	78	37.8
15	4	30	200	80	38.1
16	4	40	100	80	38.1
Mean (T_m)				**74.3**	**37.4**
As-Cast Al (control)				**66**	

3.3 Optimization of Sand Mold Factors for Hardness of Aluminum Alloy

This analysis provided signal-to-noise ratios and main effect plots for the mean of means and the mean of signal-to-noise ratios, as presented in the discussions below. The higher-the-better objective function was used to observe the optimum and the most influential factors in the sand mold for the production of aluminum alloy.

3.3.1 Effect of Metal Chips Type, Content, and Particle Size on Hardness.

The effect of the type of metal chip, chip content, and the chip particle size on the hardness properties of the aluminum alloy is shown in Figures 3 to 5.

3.3.1.1 Metal Chips Type on Hardness

Figure 3 shows the variation of hardness with the type of metal chips. The graph demonstrates an apparent linear increase in both hardness value and hardness signal-to-noise (S/N) ratio as the chip type progresses from Type 1(cast iron) to Type 4 (brass). This suggests that the chip materials significantly influence the thermal and mechanical behavior of the mold during casting. The steady rise implies that Chip Type 4 (brass) possesses superior thermal conductivity and compatibility with the sand matrix, promoting faster heat extraction, finer microstructure, and improved hardness. Conversely, Chip Type 1 (cast) likely offers the least enhancement due to lower thermal efficiency or poor integration with the mold. The findings and trends are similar and in agreement with the result of the works conducted by many other researchers who reported increased in mechanical properties of casting as a result of the incorporation of different conducting metals into sand mold, mainly in the form of chills for instance, Anil Kumar *et al*. [41] reported that hardness and tensile strength values of nickel-base matrix alloy fused with garnet increased. They asserted that the microstructure reveals fine grains because of the cryogenic effect. The figure shows an optimum hardness of 78.75 R_B at a brass chips content of 20 wt%.

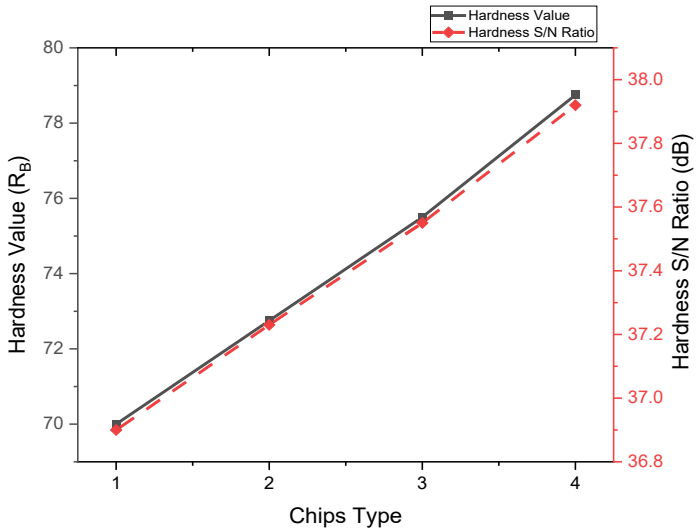

Figure 3: Variation of Hardness with metal Chips type

3.3.1.2 Metal Chip Content on Hardness

Figure 4 shows the variation of hardness with metal chip content. The figure shows that increasing the metal chips content in the molding sand from 10 wt% to 30 wt% leads to a steady rise in both hardness value and hardness signal-to-noise (S/N) ratio, indicating improved mechanical performance. This improvement is likely due to the enhanced thermal conductivity of the mold, which accelerates cooling during solidification, resulting in a finer grain structure and increased hardness. However, at 40 wt%, both hardness and S/N ratio drop sharply, suggesting that excessive chips disrupt the sand matrix, reduce compaction quality, and impair heat dissipation, potentially causing casting defects. The figure shows an optimum hardness of 75.75 R_B at a chip content of 30 wt%.

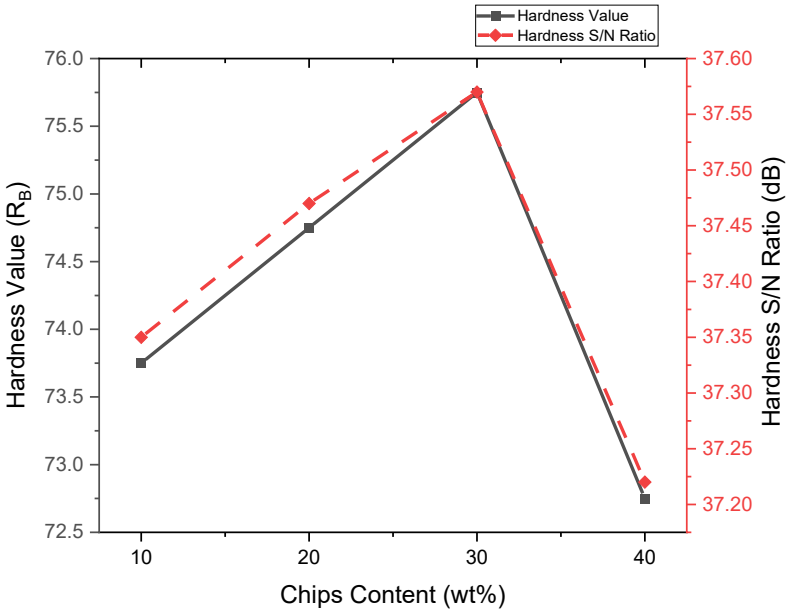

Figure 4: Variation of Hardness with Chip Content

3.3.1.3 Chips Particles Size on Hardness

Figure 5 shows the variation of hardness with the size of chip particles. The graph shows that as the chip size increases from 100 µm to 300 µm, both the hardness value and the hardness signal-to-noise (S/N) ratio decrease significantly, reaching their lowest point at 300 µm. This trend suggests that finer chips enhance the mold's thermal conductivity and packing density, leading to better heat extraction and a finer grain structure in the casting, which improves hardness. However, larger chip sizes above 300 µm appear to reduce mold uniformity and thermal efficiency, likely causing coarser grains and reduced hardness. Interestingly, a slight improvement is observed at 400 µm, indicating a possible threshold beyond which chip size may partially recover structural balance. The trend of this result agrees with related studies by Nandagopal *et al*. [42] and Ishfaq *et al.* [2]; their studies show that as the sand particles increase above the optimum values, porosities begin to form, which reduces the material's properties. From the analysis, an optimum hardness of 76.75 R_B was observed to be the best at a chip particle size of 100 µm.

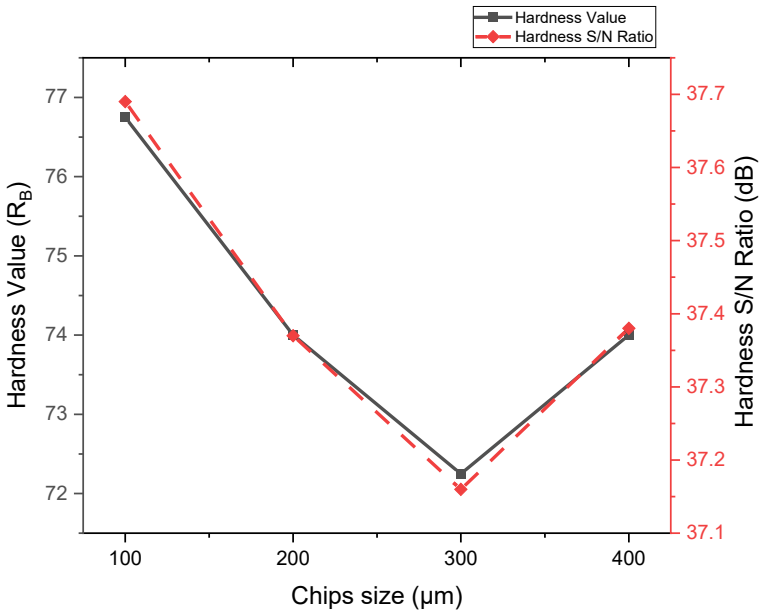

Figure 5: Variation of Hardness with Chip Particle Size

3.3.2 Optimum Combination for Hardness Value of the Aluminium Alloy

From Figure 3 to Figure 5 the optimum parameters of sand mold that give the best hardness values are: brass chips type (A) at level 4, chips content (B) at 30 %wt (level 3), and chips particle size (C) of 100 µm (level 1). Therefore, the predicted optimum combination is denoted by $A_4 – B_3 – C_1$ for hardness.

3.3.3 Estimating the Optimal Hardness.

From the analysis so far, using the optimal settings of the molding sand ($A_4 – B_3 – C_1$), an optimal hardness of 82.75 R_B for the aluminum alloy was obtained by using Equation 3.

3.3.4 Confirmation Test

The result of the hardness confirmation test is shown in Table 9. From the table, an average hardness of 83.21 RB was obtained.

Table 9: Hardness Test Confirmation Result

Runs	Factors			Hardness Value (R_B)
(S/N)	A (wt%)	B (wt%)	C (µm)	Average
1	4	30	100	83.21

The result of the predicted and the experimental hardness values of the hybrid aluminum alloy's optimal processing parameters ($A_4 – B_3 – C_1$) are shown in Table 10**,** where the error percentage is also calculated. The minimal percentage errors of 0.55% for hardness demonstrate excellent agreement between the predicted and experimental results, confirming the reliability and robustness of the optimization model. This close correlation suggests that the selected process parameters effectively enhance the mechanical performance of the cast product, validating their practical applicability for achieving high hardness in the modified sand casting process [43].

Table 10: Confirmatory Results Comparison at the Optimal Level

	Optimal process parameter settings	Predicting value (R_B)	Experimental value (R_B)	Error (%)
S/N ratio (dB)	$A_4 – B_3 – C_1$	38.38	38.40	0.05
Hardness (HB)		82.75	83.21	0.55

3.3.5 Regression Analysis (modeling)

Table 11 shows the ANOVA results obtained for the hardness of the aluminum alloy. From the table, at the significant level of 0.05, the regression model, A, B, C, and all the interactions are significant with a p-value less than 0.05.

Table 11**:** Analysis of Variance of Hardness (HD) for the Aluminium Alloy

Source	DF	Adj SS	Adj MS	F-Value	p-Value	% Contribution
Regression	6	235.72	39.29	67.00	0.000	
A	1	41.65	41.65	71.04	0.000	38.30
B	1	8.55	8.55	14.59	0.004	7.86
C	1	6.54	6.54	11.15	0.009	6.01
B^2	1	16.00	16.00	27.29	0.001	14.71
C^2	1	20.25	20.25	34.53	0.000	18.62
A*C	1	10.47	10.47	17.86	0.002	9.63
Error	9	5.28	0.59			4.85
Total	**15**	**108.75**				**100**

The predictive mathematical model for the hardness value is presented in Equation 6.

$$HD = 66.26 + 5.627A + 0.382B - 0.0390C - 0.01000\,B^2 + 0.000113\,C^2 - 0.01091\,AC \quad (6)$$

The developed regression model for hardness has a high coefficient of determination (R-square (R^2), R-square (adj), and R-square (pred) values of 97.81%, 96.35%, and 91.33%, respectively. These values show a good fit between hardness values and the factors considered for sand molding since they are close to 100%. Dan-Asabe *et al*. [44] and Sivaiah and Chakradh [33] show that an R-Square value of greater than 75% is deemed adequate. This model is suitable for prediction within and outside the range of experimental variables since the difference between the adjusted R-square and the predicted R-square is less than 20% [44-45]. Figure 6 illustrates the close agreement between the predicted and experimental fatigue strength values across 16 runs.

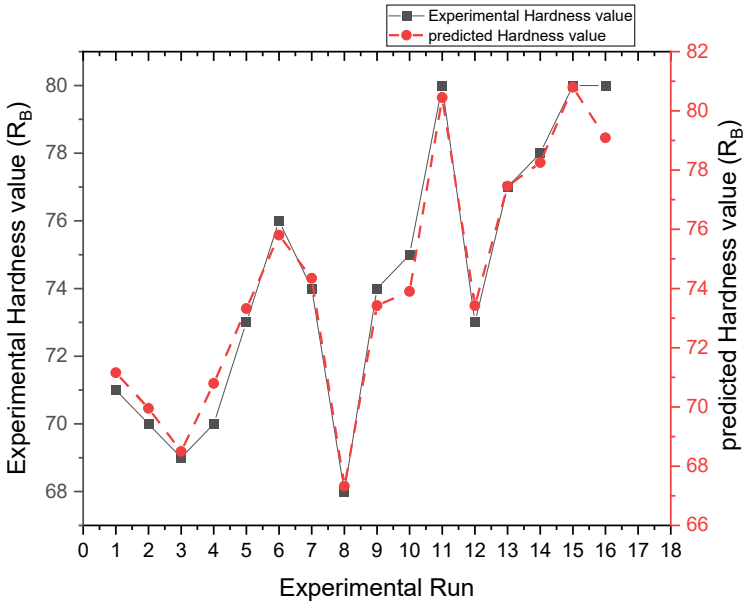

Figure 6: Experimental and Simulated (Modeled) Hardness Value

3.3.6 Confidence Interval (CI)

A confidence interval of ± 3.6 was evaluated using Equation 4. The hardness value obtained from the confirmatory test shows that the experimental value (83.21 R_B) lies between the confidence interval range of the hardness as shown below:

$$HB_{predictive} - CI < HB_{experimental} < HB_{predictive} + CI$$
$$79.61 < HB_{experimental} < 86.81$$

This result confirms the acceptability of the optimum hardness value prediction within the confidence interval of 95%.

3.4 Foundry properties of optimal molding sands

Figure 7 presents the results of the compactibility strength (COM), green compressive strength (GCS), and dry compressive strength (DCS) of the control and optimal foundry sand that were used for the production of control and optimal aluminum alloy for the hardness test. The foundry sand without the metal chips used in casting control aluminum samples for mechanical testing exhibited green compressive strength, dry compressive strength, and compactibility of 57.75 kN/m^2, 220 kN/m^2, and 44%, respectively. while 67.02 kN/m^2, 260 kN/m^2, and 47%, for the optimal foundry sand. From the analysis, the

strengths and compactibility fall within the acceptable range for aluminum alloy casting, as Sahoo *et al.* [46] (2020 and Guma [47] (2012 stipulated.

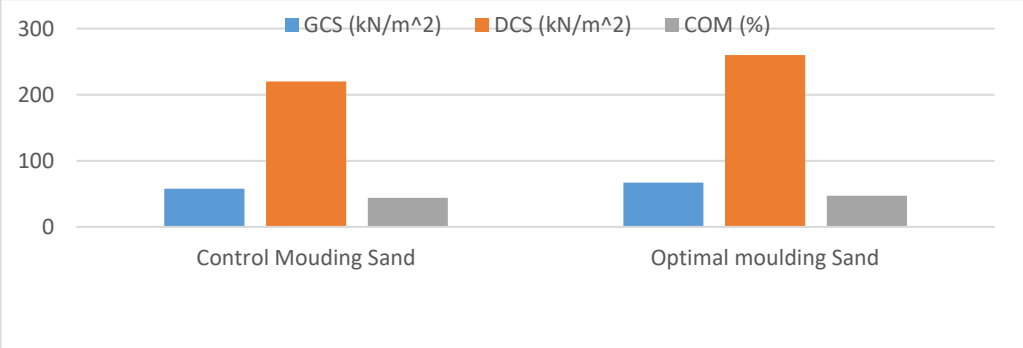

Figure 7: Foundry properties of control and optimal molding sands

3.5 SEM of the optimal and control cast aluminum alloy

Figure 8(a) and (b) show SEM images of the optimal and control samples. The gray areas represent the aluminum alloy, while the white and dark regions indicate Si-eutectoid phases, as described by Mourad *et al.* [48] and Ibrahim and Yawas [8]. The optimal sample has a much finer grain structure than the control, which likely explains its higher hardness (83.21 RB) than the control sample (66 RB).

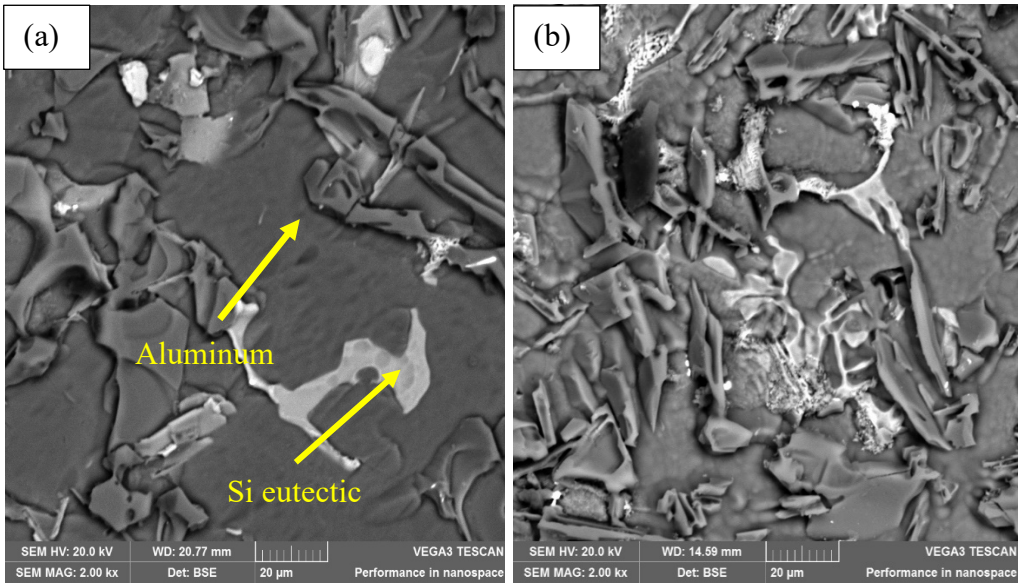

Figure 8: (a) SEM of the optimal sample and (b) SEM of the control sample

3.6 Thermal analysis of the optimal cast aluminum alloy

The thermo-gravimetric and differential thermo-gravimetric analyses (TGA/DTA) curves shown in Figure 9 reveal a two-step weight loss behavior for the optimal and the as cast aluminum alloy when heated from 30 °C to 1000 °C under a nitrogen atmosphere, indicating distinct decomposition events corresponding to moisture loss and subsequent thermal degradation of alloy constituents.

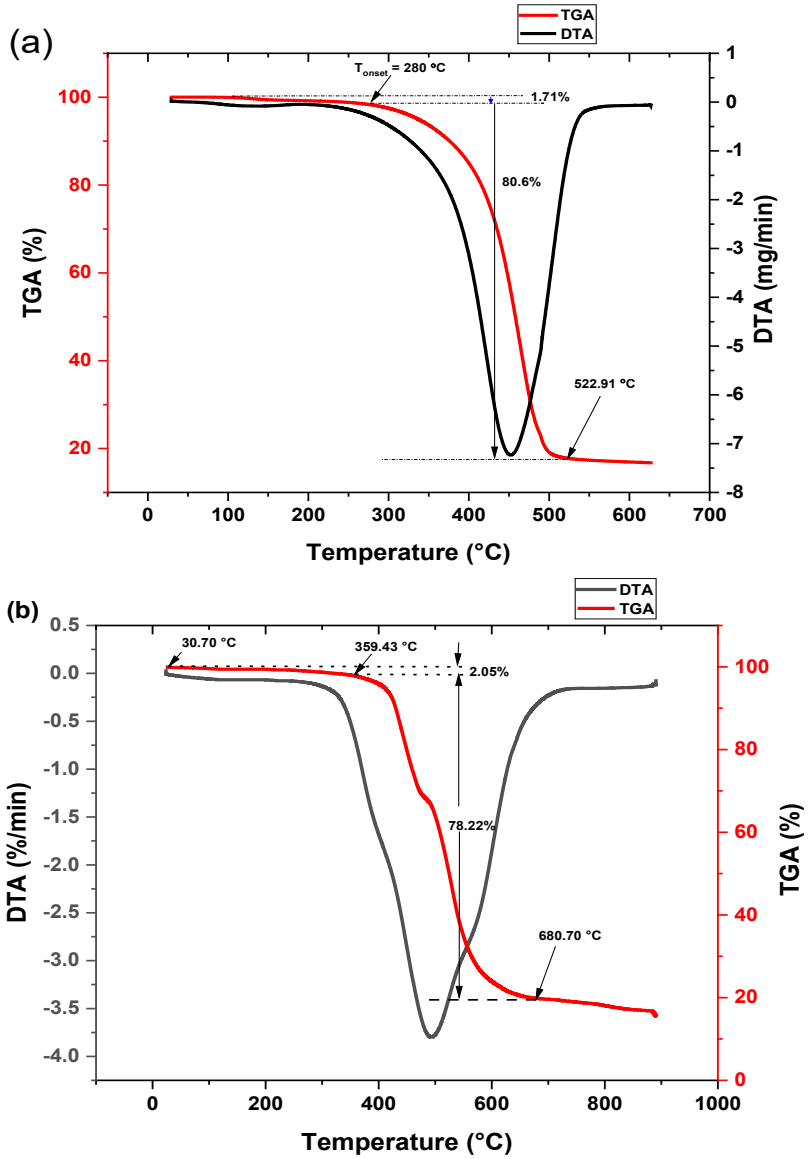

Figure 9: TGA-DTA curves showing thermal decompositions of the control and optimal cast aluminum alloy

The thermogravimetric analysis (TGA) revealed initial weight losses of 1.71% and 2.05% in the control and optimal cast aluminum alloy samples, respectively, attributed to the evaporation of surface-absorbed moisture. The major decomposition phase for the control sample occurred between 280°C and 522.62°C, with a total mass loss of 80.61%. In contrast, the optimal sample decomposed between 359.43°C and 680.70°C, with a slightly lower mass loss of 78.22%, as shown in Figure 9(b). The observed thermal decomposition is likely associated with the oxidation or volatilization of alloying elements, residual moisture, impurities, and the transformation of intermetallic phases. The onset temperature for thermal degradation was notably higher for the optimal sample (359.43°C) compared to the control (280°C), indicating improved thermal stability. Based on residual mass, the optimal cast aluminum alloy demonstrated a 12.99% enhancement in thermal stability. In terms of onset temperature, it exhibited 28.37% greater resistance to thermal degradation, confirming the beneficial effect of brass chip addition on the thermal behavior of the casting.

4.0 CONCLUSION

Based on the findings, the following conclusions can be drawn:

i. The XRF analysis confirmed the elemental composition of the materials used in the study**.** The aluminum alloy (engine block) was rich in aluminum, silicon, and magnesium. Brown sand contained a high percentage of silicon along with phosphorus and potassium. Cast iron was primarily composed of iron, carbon, and silicon, while brass showed significant amounts of copper, zinc, and iron.

ii. The highest hardness value of 80 RB was obtained in Runs 11, 15, and 16, showing a 21.2% improvement over the as-cast aluminum alloy (66 RB), while the lowest value of 68 RB was recorded in Run 8.

iii. The Taguchi optimization identified the optimal parameters as chip type at level 4 (brass), chip content at level 3 (30 wt%), and particle size at level 1 (100 μm), resulting in a 26.08% increase in hardness of the cast aluminum alloy compared to the as-cast sample. The regression model developed for predicting hardness demonstrated excellent accuracy, with R^2, adjusted R^2, and predicted R^2 values of 97.81%, 96.35%, and 91.33%, respectively. Thermogravimetric and differential thermal analyses (TGA/DTA) showed that the optimal cast aluminum alloy exhibited 12.99% higher residual mass and a 28.37% increase in onset temperature. The SEM analysis of the optimized sample revealed significant grain refinement relative to the control.

iv. The optimal foundry sand (with brass chips) showed percentage improvements of 16.03% in green compressive strength (from 57.75 to 67.02 kN/m²), 18.18% in dry compressive strength (from 220 to 260 kN/m²), and 6.82% in compactibility (from 44% to 47%) compared to the control foundry sand (without metal chips).

From an industrial perspective, incorporating metallic machining chips into molding sand offers a cost-effective and sustainable method to enhance the mechanical and thermal performance of aluminum alloy castings. This approach can be easily implemented in existing foundries using conventional equipment and machining waste, leading to improved hardness, mold strength, wear resistance, and component durability. It also reduces casting defects and supports waste minimization, aligning with SDG 9 (Industry, Innovation, and Infrastructure) and SDG 12 (Responsible Consumption and Production). Overall, this technique provides a practical and eco-friendly pathway for foundries to improve casting quality, extend product lifespan, and promote circular material utilization in sustainable manufacturing

ACKNOWLEDGEMENT

I am deeply grateful to my thesis supervisors, Prof. D. S. Yawas, Prof. T. Ause, and Prof. M. O. Afolayan, for their steadfast support, expert guidance, and invaluable encouragement throughout the course of this research. Their insightful feedback and thoughtful mentorship have played a critical role in shaping the quality and direction of this work. I sincerely appreciate their dedication and the profound impact they have had on my academic journey.

CONFLICT OF INTEREST

The author declares that there is no conflict of interest regarding the publication of this paper.

REFERENCES

1. Purba RH, Kusumoto K, Shimizu K, Efremenko V. Erosive wear behavior of novel hybrid multicomponent cast alloys with different C and B contents. Lubricants. 2023;11(6):243. doi:10.3390/lubricants11060243.
2. Ishfaq K, Ali MA, Ahmad N, Zahoor S, Al-Ahmari AM, Hafeez F. Modelling the mechanical attributes (roughness, strength, and hardness) of Al-alloy A356 during sand casting. Materials. 2020;13(3):598. doi:10.3390/ma13030598.
3. Hafeez F, Ahmed N, Ali MA, Farooq MU, AlFaify AY, Rehman AU. A comprehensive efficiency evaluation of conventional and ablation sand casting on the example of the AlSi7Mg alloy impeller. Int J Adv Manuf Technol. 2022;121(5-6):3653–72. doi:10.1007/s00170-022-09538-w.
4. Zheng Q, Zhang B, Chen T, Wu J. Achieving superior grain refinement efficiency for Al–Si casting alloys through a novel Al–La–B grain refiner. J Mater Res Technol. 2024;30:52–60. doi:10.1016/j.jmrt.2024.03.070.
5. Joshua AG, Jimoh OR. Influence of sand mould additives on tensile properties of aluminium (6061) alloy cooled in different media. Am J Mech Ind Eng. 2022;7(5):77–83.
6. Aguiar I, Cunha S, Aguiar J. Application of foundry wastes in eco-efficient construction materials: A review. Appl Sci. 2024;15(1):10. doi:10.3390/app15010010.
7. United Nations. Sustainable development goal 13: Take urgent action to combat climate change and its impacts. United Nations; 2015. Available from: https://sdgs.un.org/goals/goal13.
8. Ibrahim TK, Yawas DS. Multifaceted analysis of aluminum–coal ash–pumice composites for enhanced brake disc specific heat capacity. Jurnal Mekanikal. 2025;48:22–40. doi:10.11113/jm.v48.509.
9. Seidu SO, Kutelu BJ. Effects of additives on some selected properties of base sand. J Miner Mater Charact Eng. 2014;2(5):507.
10. Radkovský F, Gawronová M, Merta V, Lichý P, Kroupová I, Nguyenová I, et al. Effect of the composition of hybrid sands on the change in thermal expansion. Materials. 2022;15(17):6180. doi:10.3390/ma15176180.
11. Oguntuyi SD, Nyembwe K, Shongwe MB, Kabasele J, Mojisola T. A review of the influence of sand properties on parts manufactured by rapid sand casting through additive manufacturing. Int J Adv Manuf Technol. 2025;136(5-6):1989–2002. doi:10.1007/s00170-024-14979-6.
12. Vasková I, Varga L, Prass I, Dargai V, Conev M, Hrubovčáková M, et al. Examination of behavior from selected foundry sands with alkali silicate-based inorganic binders. Metals. 2020;10(2):235. doi:10.3390/met10020235.
13. Zych J, Mocek J, Snopkiewicz T, Jamrozowicz Ł. Thermal conductivity of moulding sand with chemical binders, attempts of its increasing. Arch Metall Mater. 2015;60(1):351–7. doi:10.1515/amm-2015-0058.
14. Koroyasu S. Effect of sand material type on heat absorbing properties of mold in expendable pattern casting process of aluminum alloy castings. Mater Trans. 2025;66(4):426–33. doi:10.2320/matertrans.f-m2024815.
15. Nyiramigisha P, Komariah, Sajidan. Harmful impacts of heavy metal contamination in the soil and crops grown around dumpsites. Rev Agric Sci. 2021;9(0):271–82. doi:10.7831/ras.9.0_271.
16. Hagelüken C, Lee-Shin J, Carpentier A, Heron C. The EU circular economy and its relevance to metal recycling. Recycling. 2016;1(2):242–53. doi:10.3390/recycling1020242.
17. Lee CM, Choi YH, Ha JH, Woo WS. Eco-friendly technology for recycling of cutting fluids and metal chips: A review. Int J Precis Eng Manuf-Green Technol. 2017;4(4):457–68. doi:10.1007/s40684-017-0051-9.
18. Kumar V, Tyagi SK, Kumar K, Parmar RS. Heavy metal-induced pollution in the environment through waste disposal. Int J Res Publ Rev. 2023;4(7):1205–10.
19. Emamian A. A study on wear resistance, hardness and impact behaviour of carburized Fe-based powder metallurgy parts for automotive applications. Mater Sci Appl. 2012;3(8):519–22. doi:10.4236/msa.2012.38073.
20. Zhu X, Lin J, Jiang S, Cao A, Yao Y, Sun Y, et al. Study of the effects on the strengthening mechanism and wear behavior of wear-resistant steel of temperature controlling in heat treatment. Nanomaterials. 2024;14(14):1171. doi:10.3390/nano14141171.
21. Olanipekun KA. Assessment of factors influencing the development and sustainability of small scale foundry enterprises in Nigeria: A case study of Lagos State. Asian J Soc Sci Manag Stud. 2020;7(4):288–94.
22. Khandelwal H, Ravi B. Effect of molding parameters on chemically bonded sand mold properties. J Manuf Process. 2016;22:127–33. doi:10.1016/j.jmapro.2016.03.007.
23. Tabushi K, Sato H, Watanabe Y. Grain refinement performance of aluminum cast using machining chips. J Jpn Inst Light Met. 2013;63(4):147–53. doi:10.2464/jilm.63.147.
24. Samuel E, Samuel AM, Songmene V, Samuel FH. A review on the analysis of thermal and thermodynamic aspects of grain refinement of aluminum-silicon-based alloys. Materials. 2023;16(16):5639.
25. Elanchezhian C, Vijaya M. Production technology (manufacturing processes). New Delhi: Laxmi Publications Pvt Ltd; 2016.

26. Kang JW, Shangguan HL, Peng F, Xu JY, Deng CY, Hu YY, et al. Cooling control for castings by adopting skeletal sand mold design. China Foundry. 2021;18(1):18–28. doi:10.1007/s41230-021-0150-7.
27. Ibrahim T, Leva I, Iliyasu I, Yawas DS. Comparative analysis of neem and lubricating (85W90) oils as quenchants on the mechanical properties of shield metal arc welded duplex stainless steel. Int J Sci Eng Res. 2016;7(4):1825–36.
28. Ibrahim T, Yawas DS, Aku SY. Effects of shield metal arc welding techniques on the mechanical properties of duplex stainless steel. Adv Appl Res. 2013;4(5):190–201.
29. Ibrahim T, Yawas DS, Aku SY. Effects of gas metal arc welding techniques on the mechanical properties of duplex stainless steel. J Miner Mater Charact Eng. 2013;1:222–30.
30. Ibrahim TK, Yawas DS, Dan-asabe B, Adebisi AA. Manufacturing and optimization of the effect of casting process parameters on the compressive strength of aluminum/pumice/carbonated coal hybrid composites: Taguchi and regression analysis approach. Int J Adv Manuf Technol. 2023;1–1. doi:10.1007/s00170-023-10923-2.
31. Montgomery DC. Design and analysis of experiments. New York: John Wiley & Sons; 2001.
32. Samuel BO, Alabi AA, Lawal SA, Peter E, Ibrahim TK. Optimizing the effect of heat treatment on the mechanical properties (tensile strength and hardness) of *Hyphaene thebaica* nut; a machine learning and Taguchi approach. Heliyon. 2024;10(19):e38899. doi:10.1016/j.heliyon.2024.e38899.
33. Sivaiah P, Chakradhar D. Modeling and optimization of sustainable manufacturing process in machining of 17-4 PH stainless steel. Measurement. 2019;134:142–52.
34. Alabi AA, Samuel BO, Peter ME, Tahir SM. Optimization and modelling of the fracture inhibition potential of heat treated doum palm nut fibres in phenolic resin matrix polymer composite: a Taguchi approach. Funct Compos Struct. 2022;4(1):015004. doi:10.1088/2631-6331/ac5466.
35. Ibrahim TK, Yawas DS, Dan-asabe B, Adebisi AA. Taguchi optimization and modelling of stir casting process parameters on the percentage elongation of aluminium, pumice and carbonated coal composite. Sci Rep. 2023;13:2915. doi:10.1038/s41598-023-29839-8.
36. Ibrahim TK, Yawas DS, Dan-asabe B, Adebisi AA. Optimization and statistical modelling of the thermal conductivity of a pumice powder and carbonated coal particle hybrid reinforced aluminium metal matrix composite for brake disc application; a Taguchi approach. Funct Compos Struct. 2023;5:015008. doi:10.1088/2631-6331/acc0d1.
37. Ibrahim TK, Yawas DS, Thaddaeus J, Dan-asabe B, Iliyasu I, Adebisi AA, et al. Development, modelling and optimization of process parameters on the tensile strength of aluminum reinforced with pumice and carbonated coal hybrid composites for brake disc application. Sci Rep. 2024;14(1):16999.
38. Ibrahim TK, Iliyasu I, Abiodunt PC. Application of Taguchi methods and regression analysis to optimize process parameters and reinforcements for maximizing composite's coefficient of friction for brake disc application: a statistical optimization approach. J Sustain Mater Process Manag. 2024;4(1):89–105.
39. Ibrahim TK, Thaddaeus J, Popoola CA, Iliyasu I, Alabi AA. Improvement of wear rate properties of a brown pumice and coal ash particulates reinforced aluminum composite for automobile brake manufacturing through optimization and modelling. Jordan J Mech Ind Eng. 2024;18(4).
40. Ali M, Porter D, Kömi J, Eissa M, El FH, Mattar T. Effect of cooling rate and composition on microstructure and mechanical properties of ultrahigh-strength steels. J Iron Steel Res Int. 2019;26(12):1350–65. doi:10.1007/s42243-019-00276-0.
41. Anil Kumar BK, Ananthaprasad MG, GopalaKrishna K. Action of cryogenic chill on mechanical properties of nickel alloy metal matrix composites. IOP Conf Ser Mater Sci Eng. 2016;149:012116. doi:10.1088/1757-899X/149/1/012116.
42. Nandagopal M, Sivakumar K, Sengottuvelan M, Velmurugan S. Optimization of process parameters to reduce the green sand casting defects. In: Springer Proceedings in Materials. Singapore: Springer Nature; 2021. p. 655–61. doi:10.1007/978-981-15-8319-3_65.
43. Fatima A, Wasif M, Mumtaz MO. Optimization of process parameters in turning of nuclear grade steel alloy (AISI-410) for sustainable manufacture. J Eng Res. 2021;10(3A):337–46. doi:10.36909/jer.11239.
44. Dan-Asabe B, Yaro S, Yawas D, Aku S. Statistical modeling and optimization of the flexural strength, water absorption and density of a doum palm–Kankara clay filler hybrid composite. J King Saud Univ Eng Sci. 2019;31(4):385–94.
45. Rai A, Mohanty B, Bhargava R. Supercritical extraction of sunflower oil: a central composite design for extraction variables. Food Chem. 2016;192:647–59.
46. Sahoo PK, Pattnaik S, Sutar MK. Investigation of the foundry properties of the locally available sands for metal casting. Silicon. 2021;13(11):3765–75. doi:10.1007/s12633-020-00677-x.
47. Mourad AH, Christy JV, Krishnan PK, Mozumder MS. Production of novel recycled hybrid metal matrix composites using optimized stir squeeze casting technique. J Manuf Process. 2023;88:45–58. doi:10.1016/j.jmapro.2023.01.040.
48. Guma TN. Characteristic foundry properties of Kaduna river sand. Int J Eng Sci. 2012;1(11):3–8.